

Electronic structure of antiferromagnetic Dirac semimetal candidate GdIn_3

Z. X. Yin,^{1,2,*} X. Du,^{1,2,*} S. Zhang,^{3,*} C. Chen,⁴ D. Pei,⁵ J. S. Zhou,^{1,2} X. Gu,^{1,2} R. Z. Xu,^{1,2} Q. Q. Zhang,^{1,2} W. X. Zhao,^{1,2} Y. D. Li,^{1,2} Y. F. Xu,^{6,7} A. Bernevig,^{7,8,9} Z. K. Liu,^{10,11} E. K. Liu,^{3,†} Y. L. Chen,^{5,10,11,‡} and L. X. Yang^{1,2,§}

¹State Key Laboratory of Low Dimensional Quantum Physics, Department of Physics, Tsinghua University, Beijing 100084, China

²Frontier Science Center for Quantum Information, Beijing 100084, China

³Beijing National Laboratory for Condensed Matter Physics and Institute of Physics, Chinese Academy of Sciences, Beijing 100190, China

⁴Advanced Light Source, Lawrence Berkeley National Laboratory, Berkeley, California 94720, USA

⁵Clarendon Laboratory, Department of Physics, University of Oxford, Oxford OX1 3PU, United Kingdom

⁶Max Planck Institute of Microstructure Physics, 06120 Halle (Saale), Germany

⁷Department of Physics, Princeton University, Princeton, New Jersey 08544, USA

⁸Donostia International Physics Center, 20018 Donostia-San Sebastian, Spain

⁹IKERBASQUE, Basque Foundation for Science, 48009 Bilbao, Spain

¹⁰School of Physical Science and Technology, ShanghaiTech University and CAS-Shanghai Science Research Center, Shanghai 201210, China

¹¹ShanghaiTech Laboratory for Topological Physics, Shanghai 200031, China



(Received 23 May 2022; accepted 11 August 2022; published 30 August 2022)

Recently, magnetic topological quantum materials have attracted substantial research attention due to their great application potential. Here, using high-resolution angle-resolved photoemission spectroscopy and *ab initio* calculation, we systematically investigate the electronic structure of antiferromagnetic Dirac semimetal candidate GdIn_3 . According to our *ab initio* calculation, there exist two and one pair(s) of Dirac fermions in the paramagnetic and antiferromagnetic state, respectively. In the antiferromagnetic state, the magnetic Dirac semimetal phase is protected by C_{4z} rotation symmetry in the type-IV magnetic space group. Our experiment above the Néel temperature is well reproduced by the calculated band structure in the paramagnetic state, from which we identify a pair of Dirac fermions at 1.5 eV below the Fermi level. However, we do not observe the signature of electronic reconstruction in the antiferromagnetic state, suggesting a weak interaction between the localized Gd $4f$ states of spin configuration $S = 7/2\mu_B$ and the itinerant conduction electrons. Our results confirm the Dirac semimetal nature of the paramagnetic GdIn_3 and provide important insights into its antiferromagnetic Dirac semimetal phase.

DOI: [10.1103/PhysRevMaterials.6.084203](https://doi.org/10.1103/PhysRevMaterials.6.084203)

I. INTRODUCTION

Topological quantum materials represent a special family of compounds whose topologies of electronic structures are protected by the symmetries of the system and characterized by topological invariants [1–5]. Up to date, many different types of topological quantum materials have been discovered, including topological insulators, topological crystalline insulators, Dirac and Weyl semimetals, nodal line semimetals, and topological superconductors [1–5]. Among them, Dirac semimetals harbor fourfold degenerate Dirac fermions with linear dispersions along all three momentum directions, realizing a three-dimensional graphene [3,6,7]. Dirac semimetals have attracted great attention due to their unique electronic structure and exciting physical properties, such as the giant diamagnetism [8,9], quantum magnetoresistance with linear field dependence [10,11], oscillating quantum spin Hall effect [12,13], and 3D quantum Hall effect [14,15]. Moreover, Dirac semimetal can be viewed as a parent state for realizing other

novel topological quantum states, such as the Weyl semimetal hosting pairs of Weyl fermions in the bulk and unclosed Fermi arcs on the surface [7,16–21].

More recently, the combination of magnetism and topology has become an important research frontier because of its great application potential in the electronic and spintronic devices. Magnetic topological insulator and Weyl semimetals have been experimentally discovered with intriguing properties [22–30]. For a Dirac semimetal, in general, both the time-reversal symmetry (TRS) T and inversion symmetry I should be respected. The breaking of either T or I will split the Dirac fermion into a pair of Weyl fermions and drive the Dirac semimetal into the Weyl semimetal phase [7,16–21]. However, a novel magnetic Dirac semimetal phase can be stabilized by the composite symmetry of T and I even if both of them alone are broken, as verified in CuMnAs [31]. This symmetry restriction can be further released in the type-IV magnetic space groups (MSG) in which T is broken but I and the nonsymmorphic TRS $\tilde{T} = T\tau$ (the combination of T and a fractional translation operator τ that connects the black and white Bravais lattices) are preserved [30,32].

In this work, by combining *ab initio* calculation and high-resolution angle-resolved photoemission spectroscopy (ARPES), we systematically study the electronic structure of

*These authors contributed equally to this work.

†ekliu@iphy.ac.cn

‡yulin.chen@physics.ox.ac.uk

§lxyang@tsinghua.edu.cn

the rare-earth intermetallic compound GdIn_3 , a candidate of magnetic Dirac semimetal that was predicted in Ref. [30]. Our *ab initio* calculation suggests two pairs of Dirac fermions at about 30 meV above and 1.5 eV below the Fermi level (E_F), respectively. Below the Néel temperature T_N near 45 K, GdIn_3 becomes an antiferromagnetic (AFM) Dirac semimetal with a pair of Dirac fermions located along the ΓZ direction. However, our experiment at low temperature shows good agreement with the calculated results in the paramagnetic state by excluding Gd 4*f* electrons, suggesting a minor impact of the AFM ordering on the electronic structure of GdIn_3 due to the well-localized *f* electrons and the negligible interaction between *f* electrons and conduction electrons. Indeed, we observe no significant change of the measured electronic structure with decreasing temperature across the Néel temperature. Our results confirm the Dirac semimetal phase in the paramagnetic state and are informative for further exploration of the AFM Dirac semimetal phase of GdIn_3 .

II. METHODS

The single crystals of GdIn_3 were grown by a self-flux method in an Al_2O_3 crucible sealed in a quartz tube. Gd and In were mixed in a ratio of 5:95. The quartz tube was heated to 1100 °C in 1 day and kept there for 1 day, to make melting gadolinium and indium react sufficiently, then slowly cooled to 600 °C in 7 days for growing GdIn_3 single crystals. After that, the quartz tube was transferred from the muffle furnace at 600 °C to a centrifugal machine where the flux indium and GdIn_3 single crystals were separated.

High-resolution ARPES measurements were performed at beamline 4.5.2 of Stanford Synchrotron Radiation Light Source and beamline I05 of the Diamond Light Source. Data were collected with Scienta R4000 electron analyzers. The overall energy and angular resolutions were set to 15 meV and 0.2°, respectively. The samples were cleaved *in situ* and measured under ultrahigh vacuum less than 1.0×10^{-10} mbar.

The first-principles band-structure calculations of GdIn_3 were performed by the Vienna *ab initio* Simulation Package (VASP). The exchange-correlation energies were considered under Perdew-Burke-Ernzerhof-type generalized gradient approximation (GGA) [33] with spin-orbit coupling included. The cutoff energy for the plane-wave basis was set to 640 eV in all calculations. A Γ -centered Monkhorst-Pack *k*-point mesh of $10 \times 10 \times 10$ was adopted for a self-consistent charge density. In the GGA + *U* calculation for the AFM configuration, Hubbard-*U* value of *f* orbitals on Gd is chosen as 6 eV. Based on the tight-binding type Hamiltonian constructed from maximally localized Wannier functions supplied by the WANNIER90 code [34], the Fermi surfaces of bulk states were calculated with the WANNIERTOOLS package [35].

III. RESULTS AND DISCUSSION

GdIn_3 crystallizes in a cubic structure [space group $Pm\bar{3}m$ (No. 221)] with indium and gadolinium atoms locating at face centers and cubic corners, respectively, as illustrated in Fig. 1(a). Below about 45 K, GdIn_3 develops a *C*-type AFM and the magnetic unit cell adopts a tetragonal lattice with type-IV MSG $Pc4/mbm$ (No. 127.397), as schematically shown in

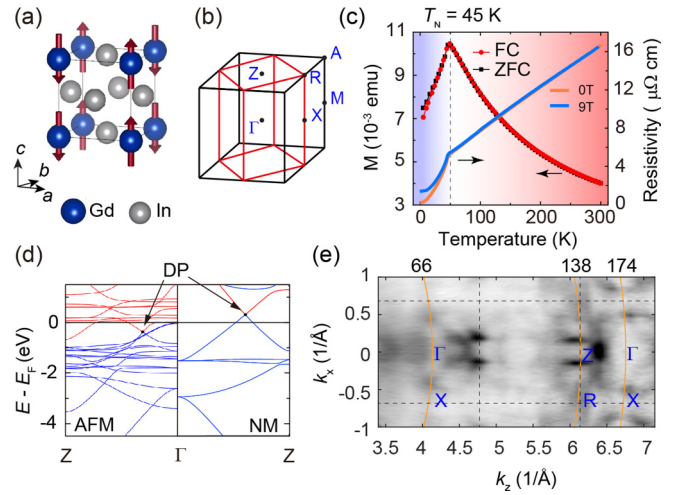


FIG. 1. Basic properties of GdIn_3 crystals. (a) Schematic of the crystal structure of GdIn_3 . The arrows indicate the alignment of magnetic moments of Gd atoms in the antiferromagnetic (AFM) state. (b) Brillouin zone (BZ) of GdIn_3 in nonmagnetic (NM) (black) and AFM (red) states. (c) Magnetization and resistivity as a function of temperature. The magnetization was measured by heating the sample under a magnetic field of 100 Oe. The sample was cooled down to 5 K under a magnetic field of 100 Oe for field-cooling (FC) and without magnetic field for zero-field cooling (ZFC) measurements, respectively. (d) *ab initio* calculated band structure along high-symmetry $Z\text{-}\Gamma\text{-}Z$ direction in the AFM and NM states. (e) Constant energy contour at 0.2 eV below E_F in $k_z\text{-}k_x$ plane. The dashed lines indicate the BZ along k_z and the yellow curves indicate the measurement directions using specified photon energies.

Fig. 1(a). Figure 1(b) shows the Brillouin zone (BZ) of GdIn_3 in nonmagnetic (NM) and AFM states. The magnetization vs temperature curve shows a peak at T_N , where the resistivity also shows an anomaly, confirming the AFM transition in our samples [Fig. 1(c)]. The generators of this MSG include I , fourfold rotation along [001] direction C_{4z} , twofold rotation along [001] direction C_{2z} , twofold screw rotation along the [100] direction $\tilde{C}_{2x} = \{C_{2x} | (\frac{1}{2}, \frac{1}{2}, 0)\}$, and an antiunitary translation symmetry $\tilde{T} = \{T | (\frac{1}{2}, \frac{1}{2}, 0)\}$, where T is TRS and $(\frac{1}{2}, \frac{1}{2}, 0)$ is a fractional translation along the [110] direction.

In the BZ of AFM phase [red lines in Fig. 1(b)], the k points along the ΓZ path preserve the magnetic little cogroup $4/m'mm$, whose elements include C_{4z} , C_{2z} , glide mirror symmetries $\tilde{M}_{2x} = \{M_{2x} | (\frac{1}{2}, \frac{1}{2}, 0)\}$ and $\tilde{M}_{2y} = \{M_{2y} | (\frac{1}{2}, \frac{1}{2}, 0)\}$. As the two glide mirror symmetries \tilde{M}_{2x} and \tilde{M}_{2y} satisfy the anticommutation relation $\{\tilde{M}_{2x}, \tilde{M}_{2y}\} = 0$, the irreducible representation (irreps) of the little group $4/m'mm$ is at least two dimensional (2D). In the band structure of GdIn_3 , as shown in Fig. 1(d), there are two 2D bands crossing below E_F along the ΓZ path. In Ref. [30], the irreps of these two bands are identified as \overline{LD}_6 and \overline{LD}_7 , respectively, whose C_{4z} eigenvalues are different. Hence, the crossing point between them is gapless and protected by the C_{4z} symmetry. As both \overline{LD}_6 and \overline{LD}_7 are 2D irreps, the gapless crossing point is 4D and behaves like a Dirac fermion that is characterized by the massless Dirac equation. Figure 1(e) shows the constant energy contour (CEC) at 0.2 eV below E_F in the $k_z\text{-}k_x$ plane. We

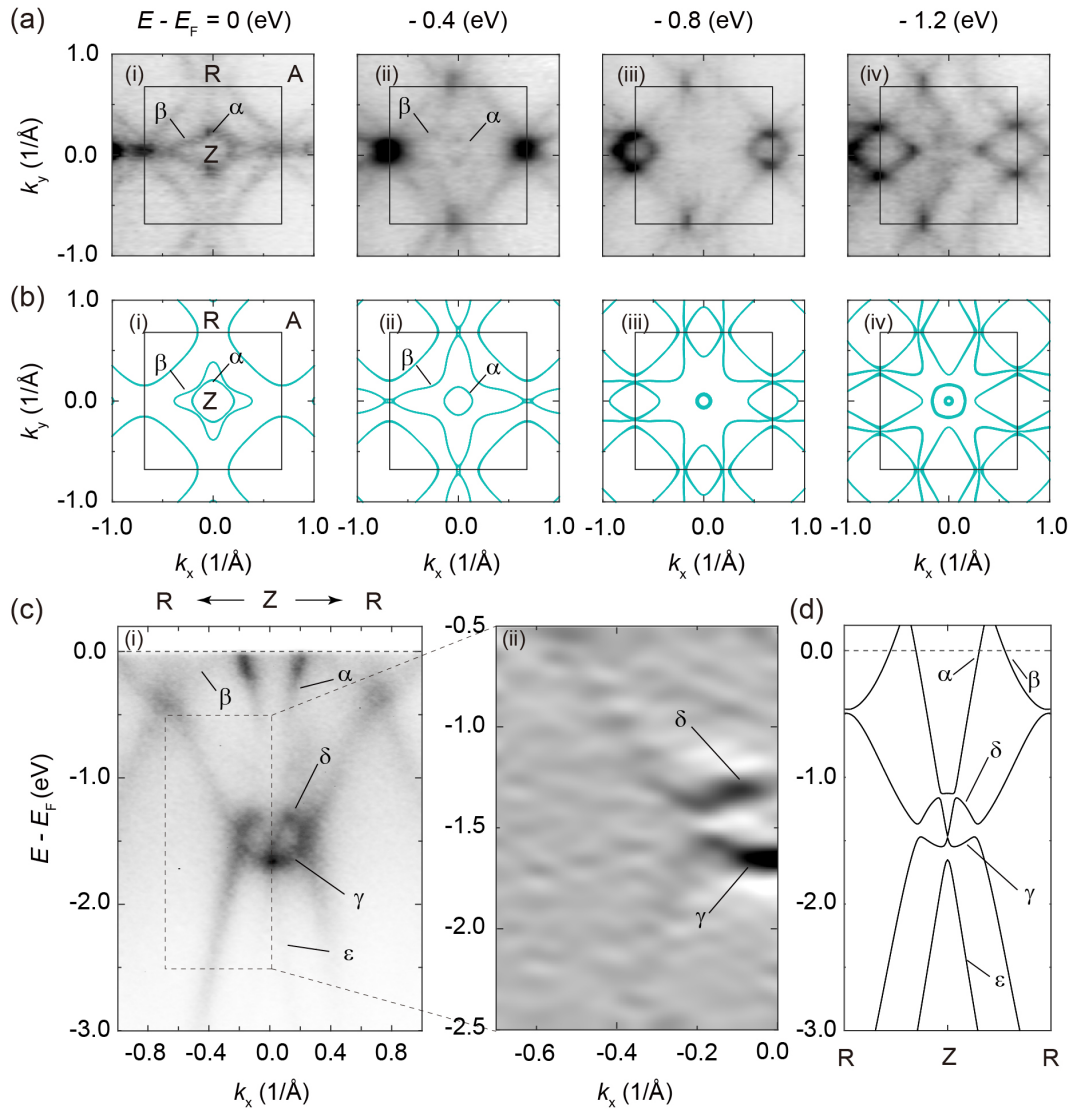


FIG. 2. Electronic structure of GdIn_3 in the R - Z - A plane. (a) Photoemission intensity map of constant energy contours (CECs) at selected binding energies. Data were integrated in an energy window of 50 meV. (b) Corresponding *ab initio* calculated results. (c), (i) Band dispersions along high-symmetry R - Z - R direction measured with left circularly polarized photons; (c), (ii) zoom-in plot of the second derivative of ARPES intensity map indicated by the rectangle in (i). Identified bulk bands are labeled. (d) Calculated band dispersions along high-symmetry R - Z - R direction. The data were collected using photons with $h\nu = 138$ eV at 65 K.

observe a periodic variation of the spectra with a periodicity of $2\pi/a$ ($a = 0.461$ nm), from which we can identify the k_z positions.

Figure 2 presents the electronic structure of GdIn_3 measured in the R - Z - A plane at 65 K. On the Fermi surface (FS), we observe an electron pocket and a four-point starlike hole pocket around the Z point, together with a large electron pocket around the A point in the BZ, as shown in Fig. 2(a). The nature of electron and hole pockets is confirmed by CECs at different binding energies [Figs. 2(a)(i)–2(a)(iv)], where the electron pocket shrinks and hole pocket expands with increasing binding energy. The observed CECs are in good agreement with our *ab initio* calculations without Gd $4f$ electrons (NM state) [Fig. 2(b)], where the electron and hole pockets around the Z point and the electron pocket around the A point are well reproduced. Figure 2(c) shows the band dispersion along the R - Z - R direction. Consistent with the FS structure, we

observe an electron band α and a hole band β crossing E_F , forming the hole and electron pockets around the Z point, respectively. Near 1.5 eV below E_F , we observe another two dispersive bands δ and γ with an energy gap between them, which can be better visualized in the second derivative of the spectra [Fig. 2(c)]. Our *ab initio* calculation without Gd $4f$ electrons (NM state) well reproduces the measured band dispersions, suggesting that the $4f$ electrons are well localized and weakly interact with the conduction electrons, in good consistency with previous measurement of de Hass-van Alphen effect [36].

Figure 3 further explores the electronic structure in the Γ - X - M plane. Similar to the band structure in the R - Z - A plane, the α and β bands cross E_F and form two Fermi pockets. The δ and γ bands, on the other hand, show much weaker dispersion. We observe extra two bands η_1 and η_2 with broadened spectral weight [Figs. 3(a) and 3(b)], which may

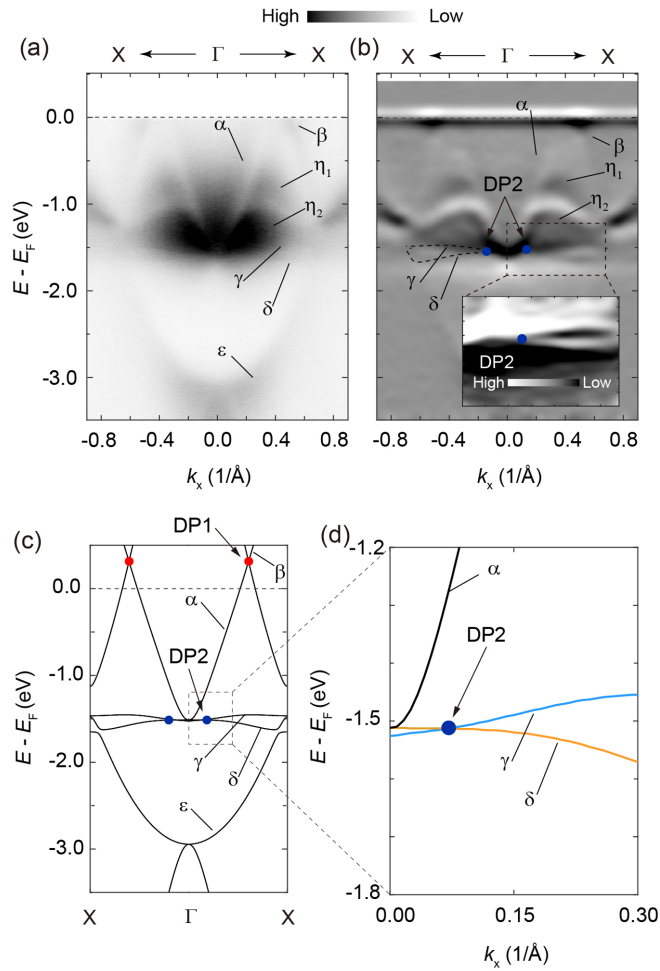


FIG. 3. Electronic structure of GdIn₃ in the Γ - X - M plane. (a) Band dispersions along high-symmetry X - Γ - X direction. (b) Second derivative of ARPES intensity map in (a). (c) *ab initio* calculated band structure along X - Γ - X , from which two pairs of Dirac points are identified. (d) Zoom-in plot of the calculated band dispersions near the Dirac point (DP2). Data were collected at 65 K.

be induced by superposition of band dispersions at different k_z values due to the finite- k_z resolution in our ARPES measurements [37]. Our experiment also shows good agreement with our *ab initio* calculation in Fig. 3(c). Our calculation reveals two pairs of Dirac points located at about 30 meV above (DP1) and 1.5 eV below (DP2) E_F [Figs. 3(c) and 3(d)], suggesting that GdIn₃ is a Dirac semimetal in its paramagnetic state. The zoom-in plot of our ARPES spectra near the Dirac points at 1.5 eV below E_F is shown in Fig. 3(b), from which we can identify the band crossing of the γ and δ bands at DP2, in good agreement with the calculation.

To investigate the influence of AFM ordering on the electronic structure of GdIn₃, we track the temperature evolution of the electronic structure across T_N in Fig. 4. Figures 4(a) and 4(b) show the band dispersion along Γ - X at selected temperatures. We do not observe clear change of the band dispersions with decreasing temperature. Moreover, the band crossing of the γ and δ bands persists to the lowest temperature. The momentum-distribution curves and energy-distribution curves at different temperatures in Figs. 4(c) and 4(d) further illus-

trate the temperature independence of the spectra. As shown in Fig. 4(e), we also do not observe any difference of the FS structure at 13 and 65 K. The temperature independence of the electronic structure of GdIn₃ suggests a negligible impact of the AFM ordering on the conduction electrons.

In an f -electron material, the interaction between localized f electrons and itinerant conduction electrons plays an essential role in the electronic and magnetic properties of the system. In the strongly correlating limit where the Kondo effect dominates, the resonant scattering between the f electrons and conduction electrons can generate a heavy band near E_F with enhanced quasiparticle mass, and results in a paramagnetic heavy fermion ground state. By contrast, in the weakly coupling limit, the local spins usually interact with each other through the Ruderman-Kittel-Kasuya-Yosida interaction and develop the long-range AFM order [38]. Our results suggest that GdIn₃ falls into the weak coupling regime, where the $4f$ electrons are well localized and their alignment shows minor influence on the conduction electrons. Therefore, the Dirac fermions in the paramagnetic state can persist into the AFM state.

On the other hand, the predicted Dirac points in the antiferromagnetic state locate along the Γ - Z direction [Fig. 1(d)] that is defined by the magnetization orientation in the system. However, the cubic structure of GdIn₃ has three equivalently preferential magnetization directions. In other words, the magnetization orientation in GdIn₃ could be along different directions in different magnetic domains, making it challenging to observe the Dirac fermions related to the antiferromagnetic state. Particularly, the surface magnetization may be different from the bulk and misaligned, which can smear the magnetic impact on the surface-sensitive ARPES spectra [23–25]. A magnetic field is thus required to align the magnetic orientation of the compound to a preferential direction to observe the Dirac point in the AFM state.

In summary, we have systematically investigated the electronic structure of the AFM Dirac semimetal candidate GdIn₃ by combining ARPES and *ab initio* calculation. The calculated results reveal Dirac semimetal phases in both the paramagnetic and AFM states. Our ARPES experiment shows good agreement with the calculation without Gd f electrons even at temperatures well below T_N , suggesting that the f electrons in GdIn₃ are well localized and the magnetic moments decouple with the Dirac fermions. Our work is important for understanding the predicted magnetic Dirac semimetal phase in the type-IV magnetic groups, which will shed light on the interplay between the magnetism and topology in magnetic topological quantum materials.

ACKNOWLEDGMENTS

This work was supported by the National Key R&D program of China (Grants No. 2017YFA0304600, No. 2017YFA0305400, and No. 2017YFA0402900), National Natural Science Foundation of China (Grants No. 11427903, No. 11774190, and No. 11634009), and EPSRC Platform Grant (Grant No. EP/M020517/1). The authors acknowledge the Diamond Light Source for the beamtime at I05 under Proposal No. SI24167-1. Use of the Stanford Synchrotron

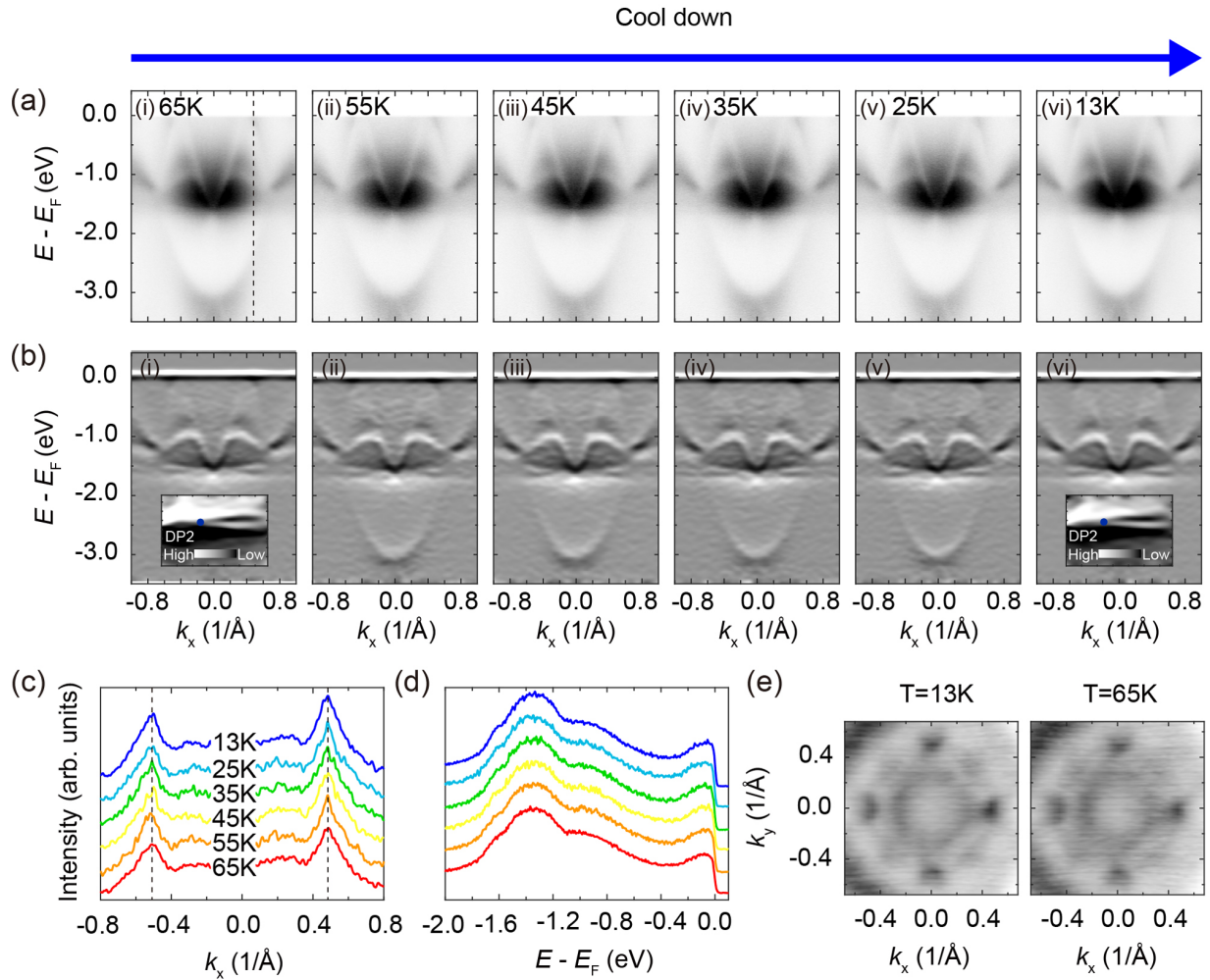


FIG. 4. Temperature evolution of the band dispersion of GdIn_3 . (a), (b) ARPES spectra along $X-\Gamma-X$ (a) and corresponding second derivative (b) at selected temperatures. (c) Temperature evolution of momentum distribution curves (MDCs) at E_F . (d) Temperature evolution of EDCs at the Fermi momentum (k_F) of the β band, indicated by the dashed line in (a)(i). (e) Comparison of the Fermi surface measured at 13 and 65 K.

Radiation Light Source, SLAC National Accelerator Laboratory, is supported by the U.S. Department of Energy, Office of

Science, Office of Basic Energy Sciences under Contract No. DE-AC02-76SF00515.

- [1] M. Z. Hasan and C. L. Kane, *Rev. Mod. Phys.* **82**, 3045 (2010).
- [2] X.-L. Qi and S.-C. Zhang, *Rev. Mod. Phys.* **83**, 1057 (2011).
- [3] N. P. Armitage, E. J. Mele, and A. Vishwanath, *Rev. Mod. Phys.* **90**, 015001 (2018).
- [4] Y. Chen, X. Gu, Y. Li, X. Du, L. Yang, and Y. Chen, *Matter* **3**, 1114 (2020).
- [5] B. Q. Lv, T. Qian, and H. Ding, *Rev. Mod. Phys.* **93**, 025002 (2021).
- [6] S. M. Young, S. Zaheer, J. C. Y. Teo, C. L. Kane, E. J. Mele, and A. M. Rappe, *Phys. Rev. Lett.* **108**, 140405 (2012).
- [7] C. He, Y. Zhang, X. F. Wang, J. Jiang, F. Chen, L. X. Yang, Z. R. Ye, F. Wu, M. Arita, K. Shimada, H. Namatame, M. Taniguchi, X. H. Chen, B. P. Xie, and D. L. Feng, *J. Phys. Chem. Solids* **72**, 479 (2011).
- [8] M. Koshino and T. Ando, *Phys. Rev. B* **81**, 195431 (2010).
- [9] P. Goswami and S. Chakravarty, *Phys. Rev. Lett.* **107**, 196803 (2011).
- [10] A. A. Abrikosov, *Phys. Rev. B* **58**, 2788 (1998).
- [11] W. Zhang, R. Yu, W. Feng, Y. Yao, H. Weng, X. Dai, and Z. Fang, *Phys. Rev. Lett.* **106**, 156808 (2011).
- [12] C.-X. Liu, H. Zhang, B. Yan, X.-L. Qi, T. Frauenheim, X. Dai, Z. Fang, and S.-C. Zhang, *Phys. Rev. B* **81**, 041307(R) (2010).
- [13] Z. Wang, Y. Sun, X.-Q. Chen, C. Franchini, G. Xu, H. Weng, X. Dai, and Z. Fang, *Phys. Rev. B* **85**, 195320 (2012).
- [14] C. M. Wang, H.-P. Sun, H.-Z. Lu, and X. C. Xie, *Phys. Rev. Lett.* **119**, 136806 (2017).
- [15] S. Li, C. M. Wang, Z. Z. Du, F. Qin, H.-Z. Lu, and X. C. Xie, *npj Quantum Mater.* **6**, 96 (2021).
- [16] S.-Y. Xu, C. Liu, S. K. Kushwaha, R. Sankar, J. W. Krizan, I. Belopolski, M. Neupane, G. Bian, N. Alidoust, T.-R. Chang,

- H.-T. Jeng, C.-Y. Huang, W.-F. Tsai, H. Lin, P. P. Shibayev, F.-C. Chou, R. J. Cava, and M. Z. Hasan, *Science* **347**, 294 (2015).
- [17] B. Q. Lv, H. M. Weng, B. B. Fu, X. P. Wang, H. Miao, J. Ma, P. Richard, X. C. Huang, L. X. Zhao, G. F. Chen, Z. Fang, X. Dai, T. Qian, and H. Ding, *Phys. Rev. X* **5**, 031013 (2015).
- [18] H. Weng, C. Fang, Z. Fang, B. A. Bernevig, and X. Dai, *Phys. Rev. X* **5**, 011029 (2015).
- [19] L. X. Yang, Z. K. Liu, Y. Sun, H. Peng, H. F. Yang, T. Zhang, B. Zhou, Y. Zhang, Y. F. Guo, M. Rahn, D. Prabhakaran, Z. Hussain, S. K. Mo, C. Felser, B. Yan, and Y. L. Chen, *Nat. Phys.* **11**, 728 (2015).
- [20] Z. K. Liu, L. X. Yang, Y. Sun, T. Zhang, H. Peng, H. F. Yang, C. Chen, Y. Zhang, Y. F. Guo, D. Prabhakaran, M. Schmidt, Z. Hussain, S. K. Mo, C. Felser, B. Yan, and Y. L. Chen, *Nat. Mater.* **15**, 27 (2016).
- [21] D. F. Liu, A. J. Liang, E. K. Liu, Q. N. Xu, Y. W. Li, C. Chen, D. Pei, W. J. Shi, S. K. Mo, P. Dudin, T. Kim, C. Cacho, G. Li, Y. Sun, L. X. Yang, Z. K. Liu, S. S. P. Parkin, C. Felser, and Y. L. Chen, *Science* **365**, 1282 (2019).
- [22] J. Li, Y. Li, S. Du, Z. Wang, B.-L. Gu, S.-C. Zhang, K. He, W. Duan, and Y. Xu, *Sci. Adv.* **5**, eaaw5685 (2019).
- [23] Y. J. Chen, L. X. Xu, J. H. Li, Y. W. Li, H. Y. Wang, C. F. Zhang, H. Li, Y. Wu, A. J. Liang, C. Chen, S. W. Jung, C. Cacho, Y. H. Mao, S. Liu, M. X. Wang, Y. F. Guo, Y. Xu, Z. K. Liu, L. X. Yang, and Y. L. Chen, *Phys. Rev. X* **9**, 041040 (2019).
- [24] X. Wu, J. Li, X.-M. Ma, Y. Zhang, Y. Liu, C.-S. Zhou, J. Shao, Q. Wang, Y.-J. Hao, Y. Feng *et al.*, *Phys. Rev. X* **10**, 031013 (2020).
- [25] H. Li, S.-Y. Gao, S.-F. Duan, Y.-F. Xu, K.-J. Zhu, S.-J. Tian, J.-C. Gao, W.-H. Fan, Z.-C. Rao, J.-R. Huang *et al.*, *Phys. Rev. X* **9**, 041039 (2019).
- [26] Y. Deng, Y. Yu, M. Z. Shi, Z. Guo, Z. Xu, J. Wang, X. H. Chen, and Y. Zhang, *Science* **367**, 895 (2020).
- [27] C. Liu, Y. Wang, H. Li, Y. Wu, Y. Li, J. Li, K. He, Y. Xu, J. Zhang, and Y. Wang, *Nat. Mater.* **19**, 522 (2020).
- [28] J. Ge, Y. Liu, J. Li, H. Li, T. Luo, Y. Wu, Y. Xu, and J. Wang, *Nat. Sci. Rev.* **7**, 1280 (2020).
- [29] H. Wang, Y. Liu, H. Zhou, H. Ji, J. Luo, J. Zhang, T. Wei, P. Wang, S. Jia, and J. Wang, *Sci. China: Phys. Mech. Astron.* **63**, 287411 (2020).
- [30] Y. Xu, L. Elcoro, Z.-D. Song, B. J. Wieder, M. G. Vergniory, N. Regnault, Y. Chen, C. Felser, and B. A. Bernevig, *Nature (London)* **586**, 702 (2020).
- [31] P. Tang, Q. Zhou, G. Xu, and S.-C. Zhang, *Nat. Phys.* **12**, 1100 (2016).
- [32] G. Hua, S. Nie, Z. Song, R. Yu, G. Xu, and K. Yao, *Phys. Rev. B* **98**, 201116(R) (2018).
- [33] J. P. Perdew, K. Burke, and M. Ernzerhof, *Phys. Rev. Lett.* **77**, 3865 (1996).
- [34] A. A. Mostofi, J. R. Yates, Y.-S. Lee, I. Souza, D. Vanderbilt, and N. Marzari, *Comput. Phys. Commun.* **178**, 685 (2008).
- [35] Q. Wu, S. Zhang, H.-F. Song, M. Troyer, and A. A. Soluyanov, *Comput. Phys. Commun.* **224**, 405 (2018).
- [36] I. Umehara, T. Ebihara, N. Nagai, Y. Fujimaki, K. Satoh, and Y. Ōnuki, *J. Phys. Soc. Jpn.* **61**, 19 (1992).
- [37] J. A. Sobota, Y. He, and Z.-X. Shen, *Rev. Mod. Phys.* **93**, 025006 (2021).
- [38] P. Coleman, *Introduction to Many-Body Physics* (Cambridge University Press, Cambridge, 2015).